

# We are IntechOpen, the world's leading publisher of Open Access books Built by scientists, for scientists

6,900

Open access books available

185,000

International authors and editors

200M

Downloads

Our authors are among the

154

Countries delivered to

TOP 1%

most cited scientists

12.2%

Contributors from top 500 universities



WEB OF SCIENCE™

Selection of our books indexed in the Book Citation Index  
in Web of Science™ Core Collection (BKCI)

Interested in publishing with us?  
Contact [book.department@intechopen.com](mailto:book.department@intechopen.com)

Numbers displayed above are based on latest data collected.  
For more information visit [www.intechopen.com](http://www.intechopen.com)



---

# Dipping Deposition Study of Anodized-Aluminum Pressure-Sensitive Paint for Unsteady Aerodynamic Applications

---

Hiroataka Sakaue

Additional information is available at the end of the chapter

<http://dx.doi.org/10.5772/57416>

---

## 1. Introduction

In aerospace engineering, anodized-aluminum pressure-sensitive paint (AA-PSP) has been used in short duration time tests [1 - 12], unsteady flow visualizations, and unsteady pressure measurements [13 - 25]. Because of its nano-open structure (Figure 1), AA-PSP yields high mass diffusion that results in a pressure response time on the order of ten microseconds [26]. This structure enables oxygen gas to interact directly with luminophores on the pore surface, which provides fast response to pressures. By applying an AA-PSP, we can obtain global surface pressure information instead of pointwise information that may result in wide applications in pressure detection fields. AA-PSP is an optical sensor that consists of a molecular pressure probe (luminophore) and an anodized aluminum as a supporting matrix. As schematically shown in Figure 2, the luminophore on the anodized-aluminum surface is excited by an illumination source and gives off luminescence. This luminescence is related to gaseous oxygen in a test gas, a process called oxygen quenching. Because the gaseous oxygen can be described as a partial pressure of oxygen as well as a static pressure, the luminescence from an AA-PSP can be described as a static pressure. See Section 3.2 for a detailed description.

The luminophore is directly related to important parameters of AA-PSPs, such as the luminescent signal level, pressure sensitivity, temperature dependency, and response time. Mainly three types of luminophores are commonly used for PSP in general, such as ruthenium complex, porphyrin, and pyrene. Each luminophore has an optimum excitation wavelength, and its peak wavelength of luminescence varies by the luminophore as well. For AA-PSP, the luminophore is applied on the anodized-aluminum surface by the dipping deposition method [27]. This method requires a luminophore, a solvent, and an anodized-aluminum coating. The

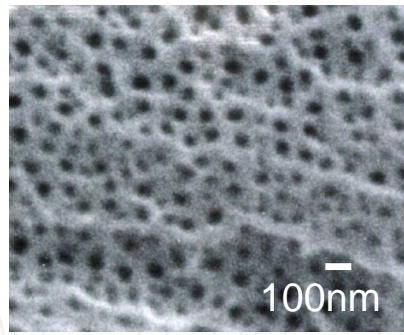


**Figure 1.** Nano-open structure of anodized-aluminum surface. Surface image was taken using a scanning electron microscope.

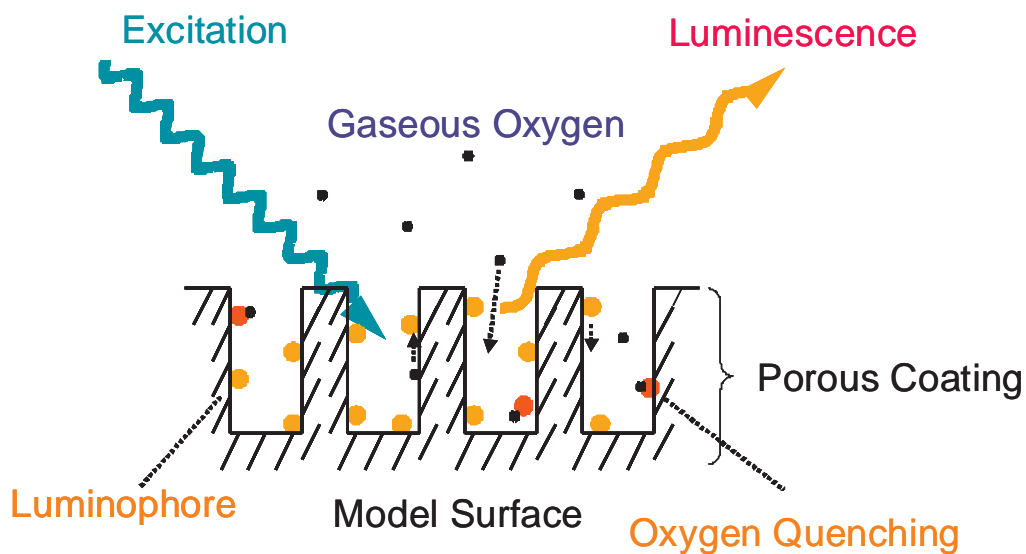


**Figure 2.** Schematic description of anodized-aluminum pressure-sensitive paint (AA-PSP).

application procedure is schematically shown in Figure 3. This method first dissolves the luminophore in solvent, and anodized-aluminum coating is dipped in the solution to apply the luminophore on the anodized-aluminum surface. However, this method was not quite understood, so that other luminophores were not successfully applied on an anodized-aluminum surface. For a given luminophore, a selection of solvent may influence to the AA-PSP characterizations: the signal level, pressure sensitivity, temperature dependency, and response time. The luminophore concentration may influence to the AA-PSP characterizations, because the amount of luminophore on an anodized-aluminum surface may change with the concentration used in the dipping deposition. The dipping duration can be another important parameter that influences the AA-PSP characterizations, because it would influence the amount of luminophore applied on the anodized-aluminum surface. The effects on the dipping duration as well as the above mentioned dipping parameters would give us fundamental knowledge to apply various luminophores on the anodized-aluminum coating. However, the effects of these parameters on AA-PSP have not been studied.

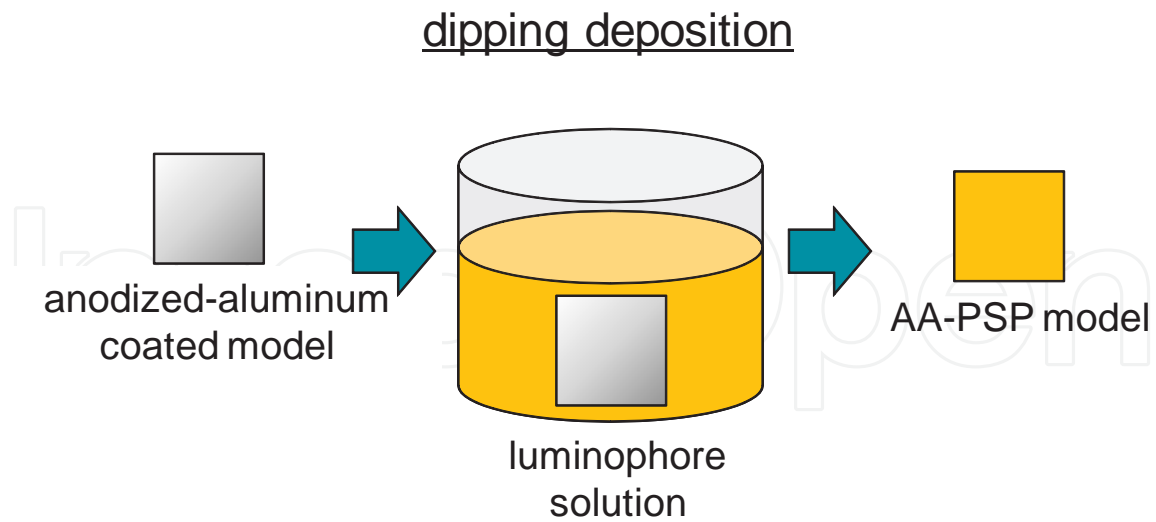


**Figure 3.** Schematic description of dipping deposition method.

In this chapter, the luminophore application method of dipping deposition is studied. This includes steady- and unsteady-state characterizations of AA-PSP, such as the signal level, pressure sensitivity, temperature dependency, and response time. The study of this method will expand our selection of luminophores onto an anodized aluminum, which will be beneficial for fabricating AA-PSP for various aerodynamic-measurement purposes especially in unsteady measurement applications.

## 2. Materials and luminophore application

Anodized-aluminum coated samples were prepared from a sheet of pure aluminum, anodization process, and cut in pieces (10 mm × 10 mm). The anodization process and the luminophore-application process were as follows. The anodization process gives an anodized aluminum of 20 nm pore size with the thickness of  $10 \pm 1 \mu\text{m}$ . The thickness was measured by an eddy current apparatus (Kett, LZ-330). Bathophen ruthenium (RuDPP) from GFS Chemicals was used as a luminophore. It is a conventional luminophore for AA-PSP.

- **Step1 Pretreatment.** An aluminum sheet was dipped in a 2% sodium hydroxide solution for 2 min to remove an excess oxidized layer. The surface was rinsed by water after this process.
- **Step2 Anodization.** A constant current density ( $10 \text{ mA/cm}^2$ ) was applied to the aluminum sheet, which was connected to anode in 1 M sulfuric acid at  $0^\circ\text{C}$ .
- **Step3 Anodized layer modification.** The anodized sheet was dipped in a 5 % phosphoric acid for 20 min at  $30^\circ\text{C}$ . After this process, the sheet was rinsed by water.
- **Step4 Luminophore application (dipping deposition).** For a given luminophore (RuDPP), the solvent polarity, luminophore concentration, and dipping duration were varied to study

the luminophore application process. After the dipping, AA-PSP was rinsed with the same solvent used. Then, remained solvents on AA-PSP samples were evaporated in a vacuum chamber at 50 °C for about 3 hours.

In total eight solvents (hexane, toluene, dichloromethane, chloroform, acetone, *N,N*-dimethyl formamide, dimethyl sulfoxide, and water) were selected for the solvent-polarity study in order from non-polar to the highest polarity index. The luminophore concentration was selected from a very dilute case of 0.001 mM to 10 mM, where the luminophore reached to its saturation. The dipping duration was varied from a very short dipping of 1 s to a very long dipping of 100,000 s (over 1 day). Even though the upper limit of the dipping duration would be infinity, the author assumed that over 1 day of dipping duration would be enough to understand the change in the AA-PSP characterizations. The reference AA-PSP, which was labeled as AAPSP<sub>ref</sub>, was created by dichloromethane as a solvent, the concentration of 0.1 mM, and the dipping duration of one hour.

To study the effect on the solvent polarity, 11.7 mg of RuDPP was dissolved in 100 ml of eight different solvents based on the polarity index (Table 1 (a)). If RuDPP is dissolved completely, the concentration was 0.1 mM. If not dissolved, the solution was saturated with excess RuDPP remained. Anodized-aluminum samples were dipped in RuDPP solutions. The dipping time was one hour at room conditions. Eight different AA-PSP samples were labeled based on their polarity index of solvents (Table 1 (a)).

To study the effect on the luminophore concentration, dichloromethane was chosen as a solvent. The concentration had the range of the fifth order of magnitude; it was varied from 0.001 mM to 10 mM. The dipping duration was one hour at room conditions. Table 1 (b) lists the luminophore application conditions related to the concentration. Prepared AA-PSPs were labeled (also listed in Table 1 (b) as Sample ID).

To study the effect on the dipping duration, dichloromethane was chosen as a solvent, and the concentration of the luminophore solution was fixed at 0.1 mM. The duration was varied from 1 s to 100,000 s. Table 1 (c) lists the conditions related to the dipping duration. Prepared AA-PSPs are labeled based on their dipping conditions, which are also listed in Table 1 (c) as Sample ID.

### 3. Steady-state characterization

Figure 4 schematically describes the calibration system, which consists of a spectrometer (Hitachi High Technologies, F-7000) and a pressure- and temperature-controlled chamber. This system characterizes the luminescent spectrum of an AA-PSP sample with varying pressures and temperatures. For characterization, an AA-PSP sample was placed in the test chamber. The excitation wavelength was set at 460 nm by a monochromator via a xenon lamp illumination in the spectrometer unit. The chamber has optical windows that passed the excitation from the illumination unit and the luminescence from the sample. The luminescence from AA-PSP samples was measured from 570 to 800 nm for a given pressure and a given

Sample ID	Polarity Index	Solvent
AAPSP <sub>ind00</sub>	0.1	Hexane
AAPSP <sub>ind02</sub>	2.4	Toluene
AAPSP <sub>ref</sub>	3.1	Dichloromethane
AAPSP <sub>ind04</sub>	4.1	Chloroform
AAPSP <sub>ind05</sub>	5.1	Acetone
AAPSP <sub>ind06</sub>	6.4	<i>N,N</i> -dimethylformamide
AAPSP <sub>ind07</sub>	7.2	Dimethylsulfoxide
AAPSP <sub>ind10</sub>	10.2	Water

(a)

Sample ID	Luminophore Concentration (mM)
AAPSP <sub>00.001</sub>	0.001
AAPSP <sub>00.010</sub>	0.01
AAPSP <sub>ref</sub>	0.1
AAPSP <sub>01.000</sub>	1
AAPSP <sub>10.000</sub>	10

(b)

Sample ID	Dipping Duration (s)
AAPSP <sub>1</sub>	1
AAPSP <sub>10</sub>	10
AAPSP <sub>100</sub>	100
AAPSP <sub>1000</sub>	1,000
AAPSP <sub>ref</sub>	3,600
AAPSP <sub>100000</sub>	100,000

(c)

**Table 1.** (a). Luminophore application conditions: solvent polarity. Dipping solvent was selected based on the polarity index. RuDPP concentration was fixed at 0.1 mM, and anodized-aluminum coatings were dipped at room temperature for one hour. (b). Luminophore application conditions: luminophore concentration. RuDPP concentration was varied from 0.001 mM to 10 mM. Dipping solvent was dichloromethane, and anodized-aluminum coatings were dipped at room temperature for one hour. (c). Luminophore application conditions: dipping duration. Dipping duration was varied from 1 to 100,000 s. Dichloromethane was chosen as a solvent, and RuDPP concentration was fixed at 0.1 mM.

temperature. The luminescent signal of an AA-PSP was then determined by integrating the spectrum from 600 to 700 nm. For pressure calibration, the chamber was connected to a pressure controlling unit (Druck DPI515), with settings from 5 to 120 kPa at a constant temperature at 25 °C. For temperature calibration, a sample heater/cooler was controlled to vary the temperature from 10 to 50 °C with a constant pressure at 100 kPa. The test gas was

dry air. For the signal level characterization, all the AA-PSP samples were measured with the same optical setup in the spectrometer but replacing samples in the chamber at constant pressure and temperature of 100 kPa and 25 °C, respectively. Throughout our characterizations, reference conditions were 100 kPa and 25 °C. The signal level,  $\eta$ , pressure sensitivity,  $\sigma$ , and temperature dependency,  $\delta$ , were characterized from the luminescent signals of AA-PSPs. Definitions and procedures to derive these characterizations are described in Sections 3.1, 3.2, and 3.3.

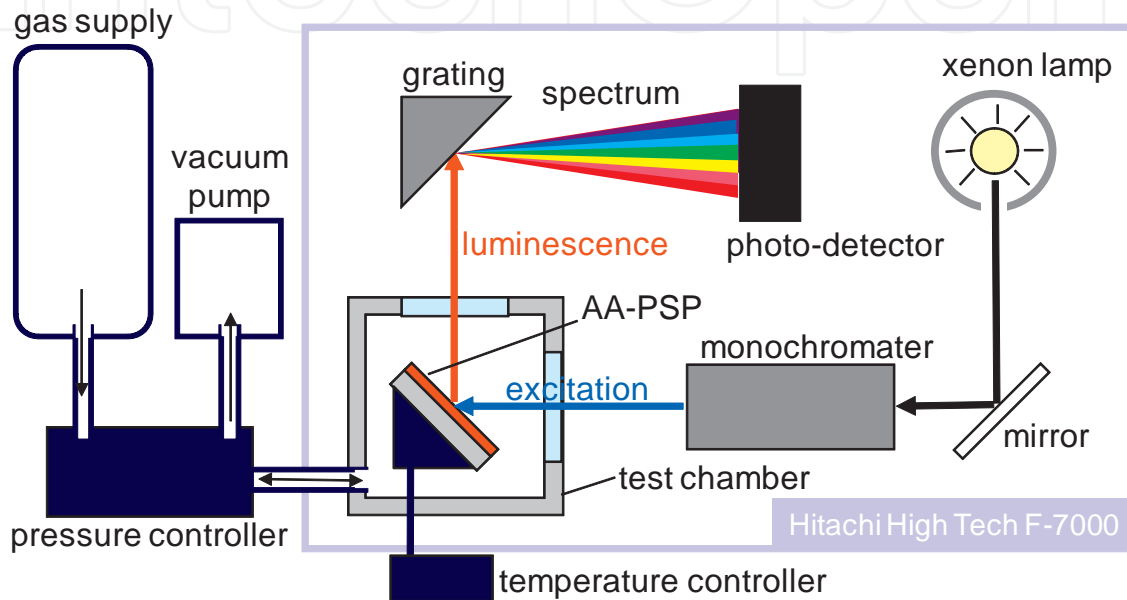


**Figure 4.** Schematic of AA-PSP calibration setup.

### 3.1. Signal Level

The luminescent signal,  $I$ , was determined by the integration of AA-PSP spectrum from 600 to 700 nm. Based on Liu *et al.*, this can be described by the gain of the photo-detector in our spectrometer,  $G$ , the emission from AA-PSP,  $I_{AAPSP}$ , the excitation in the spectrometer,  $I_{ex}$ , and the measurement setup component,  $f_{set}$  [28]:

$$I = GI_{AAPSP}I_{ex}f_{set} \quad (1)$$

In our calibration setup,  $G$ ,  $I_{ex}$ , and  $f_{set}$  were the same for all AA-PSP samples. We non-dimensionalized the luminescent signal by that of AAPSP<sub>ref</sub>  $I_{AAPSPref}$ . All luminescent signals were determined at the reference conditions. We call this value as the signal level,  $\eta$ , shown in Equation (2):

$$\eta = \frac{I}{I_{AAPSPref}} (\%) \quad (2)$$

### 3.2. Pressure sensitivity

Based on the Stern-Volmer relationship, the luminescent intensity,  $I$ , is related to a quencher [29]:

$$\frac{I_0}{I} = 1 + K_q[O_2] \quad (3)$$

Where  $I_0$  is the luminescent intensity without quencher and  $K_q$  is the Stern-Volmer quenching constant. The quencher is oxygen, which is described by the oxygen concentration,  $[O_2]$ . For AA-PSP,  $[O_2]$  can be described by the adsorption and surface diffusion of the adsorbed oxygen on an anodized-aluminum surface. We can describe  $[O_2]$  by the partial pressures of oxygen as well as the static pressures. These are combined with Equation (3) to give the adsorption-controlled model [27]:

$$\frac{I_{ref}}{I} = A + B \left( \frac{p}{p_{ref}} \right)^\gamma \quad (4)$$

Where  $A$ ,  $B$ , and  $\gamma$  are calibration constants, respectively. Here,  $ref$  denotes our reference conditions.

Pressure sensitivity,  $\sigma$  (%), describes the change in the luminescent signal over a given pressure change. This corresponds to a slope of the Equation (4) at the reference conditions:

$$\sigma = \frac{d(I_{ref}/I)}{d(p/p_{ref})} \Big|_{p=p_{ref}} = B \cdot \gamma \quad (\%) \quad (5)$$

### 3.3. Temperature dependency

AA-PSP, like PSP in general, has a temperature dependency [30]. This influences the luminescent signal, which can be described as the third order polynomial in Equation (6):

$$\frac{I}{I_{ref}} = c_{T0} + c_{T1}T + c_{T2}T^2 + c_{T3}T^3 \quad (6)$$

Where  $c_{T0}$ ,  $c_{T1}$ ,  $c_{T2}$ , and  $c_{T3}$  are calibration constants, respectively. We defined the temperature dependency,  $\delta$ , which is a slope of the temperature calibration at the reference conditions (Equation (7)). If the absolute value of  $\delta$  is large, it tells us that the change in luminescent signal over a given temperature change is also large. This is unfavorable condition as a pressure sensor. On the contrary, zero  $\delta$  means that AA-PSP is not temperature dependent:

$$\delta = \frac{d(I/I_{ref})}{dT} \Big|_{T=T_{ref}} = c_{T1} + 2c_{T2}T_{ref} + 3c_{T3}T_{ref}^2 \quad (\% / ^\circ C) \quad (7)$$

Overall, our  $\delta_s$  showed negative (see Section 5.3). This means that  $\delta_{\min}$  is the most temperature dependent and  $\delta_{\max}$  the least temperature dependent.

#### 4. Unsteady-state characterization

A vertical shock tube for characterizing the response time is schematically shown in Figure 5 (a). The length of the driver and driven sections are 1420 mm and 5530 mm, respectively. The driven section has a square cross section of 100 mm  $\times$  100 mm, and a test section is installed at the end of the driven section. The test gas was dry air and initially set at room conditions. When the diaphragm between the driver and the driven sections is ruptured, a planar shock wave propagates into the driven section. We set the driver pressure as 400 kPa that created a planar shock wave with the Mach number of 1.30.

The schematic description of the test section is shown in Figure 5 (b). An AA-PSP sample was fixed on a flat plate placed on the bottom wall of the shock tube. The samples were illuminated by a continuous 400 nm laser. A planar shock wave and its normal reflection created a step change of pressure. A photomultiplier tube (PMT, Hamamatsu R7236) was used to detect the intensity change of luminescence from the AA-PSP sample through a 605  $\pm$  40 nm band-pass filter. The output signal from the PMT was amplified by Hamamatsu C1053-03 through an analog low-pass filter with a cutoff frequency of 1 MHz. The filtered signal was then digitized to 12 bits and sampled on an A/D converter (Yokogawa, DL1540C) at a rate of 200 MHz [31].

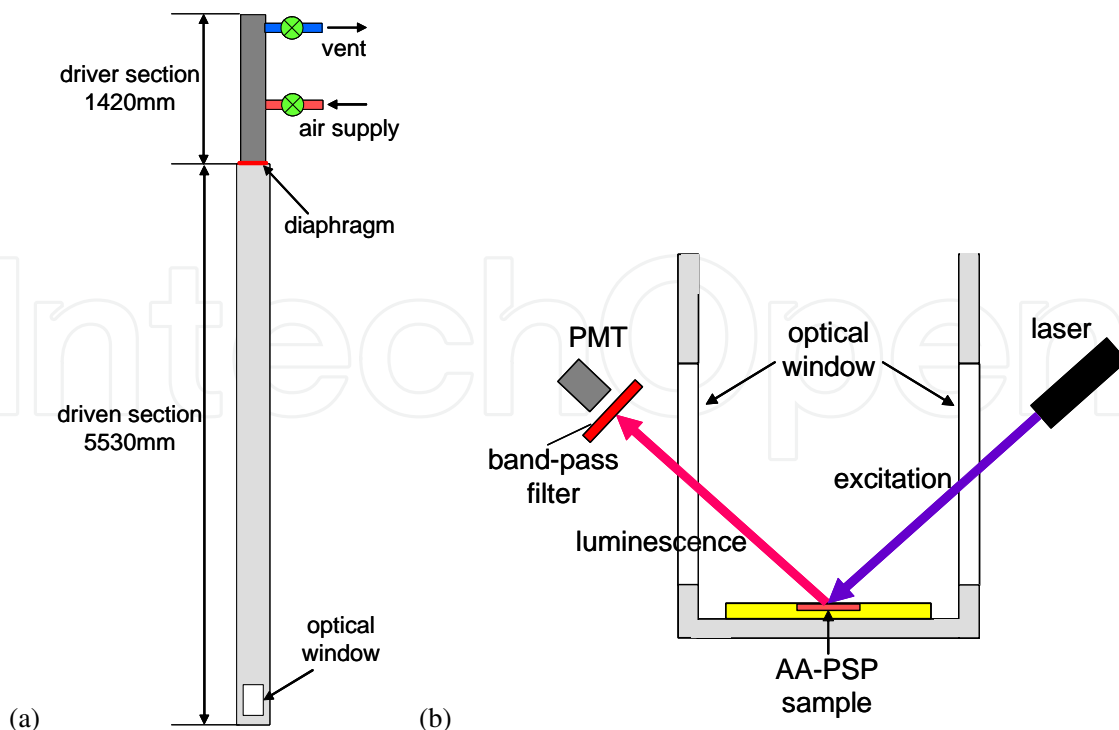


**Figure 5.** (a). Schematic description of shock tube. (b). Test section and optical setup of the shock tube.

#### 4.1. Response time

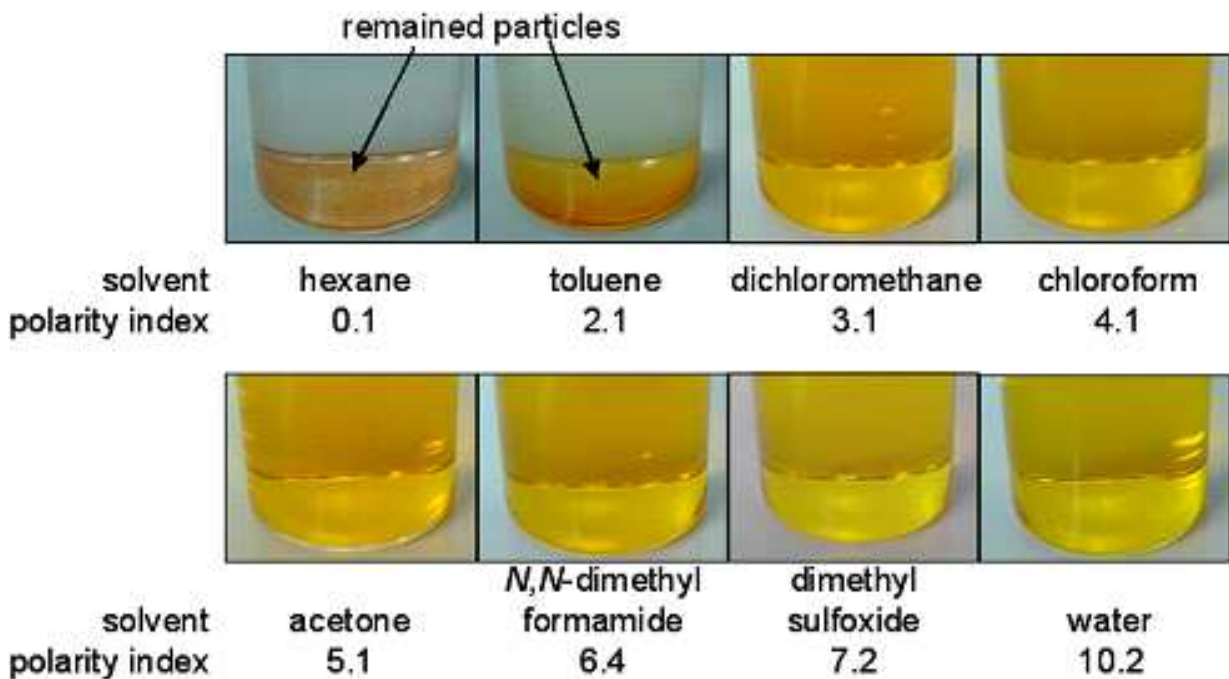
The luminescent signal was converted to a normalized pressure,  $p_{norm}$  to characterize the response time, derived from Equation (8).

$$p_{norm} = \frac{p - p_{min}}{p_{max} - p_{min}} = \frac{(I_{ref} / I - A)^{1/\gamma} - (I_{ref} / I_{min} - A)^{1/\gamma}}{(I_{ref} / I_{max} - A)^{1/\gamma} - (I_{ref} / I_{min} - A)^{1/\gamma}} \quad (8)$$

Where *min* and *max* denote the minimum and maximum values of a step change, respectively. We used the 90 % rise of  $p_{norm}$  to determine the response time.

### 5. Characterization results

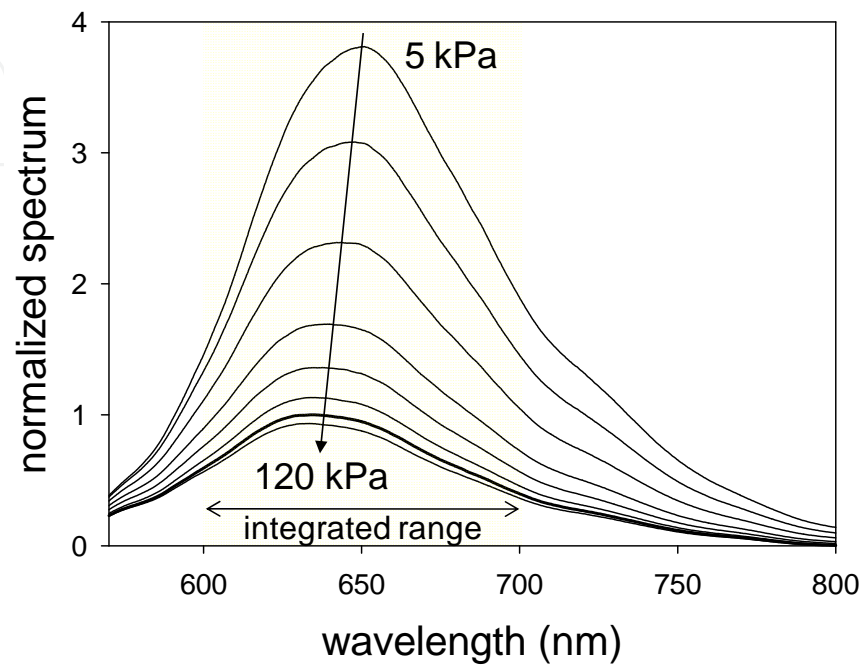
Photographs of RuDPP solution were taken to qualitatively verify the solubility of RuDPP (Figure 6). All solvents dissolved RuDPP except for the solvent with lowest polarity index (hexane). Toluene, which was the second lowest solvent in our test, partially dissolved RuDPP. Water, which gave the highest polarity index in our test, partially dissolved RuDPP, but it dissolved RuDPP completely after about one day. Other solvents dissolved RuDPP as soon as RuDPP particles were dropped to the solvents.



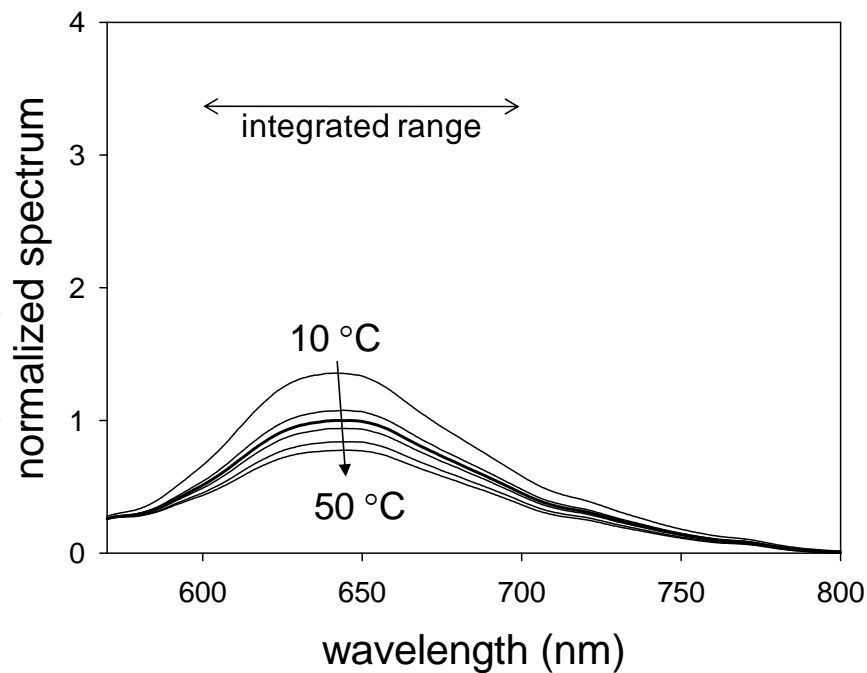
**Figure 6.** RuDPP dissolved in solvents with range of polarity index.

Figure 7 (a) and (b) show luminescent spectra of AAPSP<sub>ref</sub> with varying pressures and temperatures, respectively. Spectra were normalized by the luminescent peak at the reference

conditions. We can see that, as increasing the pressure, the luminescent spectrum decreased due to oxygen quenching [29]. As the temperature increases, we can see the spectrum decreased due to the thermal quenching [29]. It was noticed that the luminescent peak was shifted



(a)



(b)

**Figure 7.** (a). Pressure spectra of AAPSP<sub>ref</sub>. Thick line shows the spectrum at reference conditions of 100 kPa and 25 °C. (b). temperature spectra of AAPSP<sub>ref</sub>. Thick line shows the spectrum at reference conditions of 100 kPa and 25 °C.

from 650 to 635 nm by increasing the pressure from 5 to 120 kPa. For temperature spectra, the peak was shifted from 640 to 645 nm by increasing the temperature from 10 to 50 °C. As described in Section 3, we integrated an obtained spectrum from 600 to 700 nm to determine as the luminescent intensity,  $I$ , for a given pressure and a temperature.

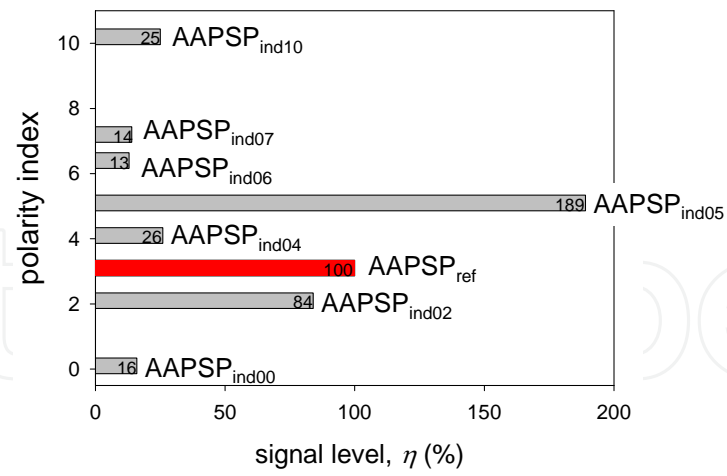
### 5.1. Luminescent signal

The signal level,  $\eta$ , was determined from Equation (2). Figure 8 (a) shows the signal level,  $\eta$ , related to the polarity index, normalized by the signal of AAPSP<sub>ref</sub> at 100 kPa. The  $\eta$  was shown as a bar with the determined value. It is obvious that the luminophore application method of dipping deposition greatly influenced the signal level. AAPSP<sub>ind00</sub> from the polarity index of 0.1 (hexane) showed very low RuDPP application on anodized aluminum, indicated by the signal level. Note that hexane did not dissolve RuDPP (Figure 6). AAPSP<sub>ind02</sub> from the polarity index of 2.4 (toluene) applied RuDPP well on anodized aluminum, which can be seen from the signal level. Here, toluene partially dissolved RuDPP. As increasing polarity index, RuDPP applied on anodized aluminum. However, the application suddenly dropped between polarity index at 6.4 of *N, N*-dimethyl amide and at 7.2 of dimethyl sulfoxide. The application brought back at the highest polarity index of 10.2 (water). The highest signal level of 1.89 was obtained from AA-PSP<sub>ind05</sub>. It can be said that a range of polarity index of solvent exists that applies RuDPP. However, this range does not correspond to the range of dissolving RuDPP.

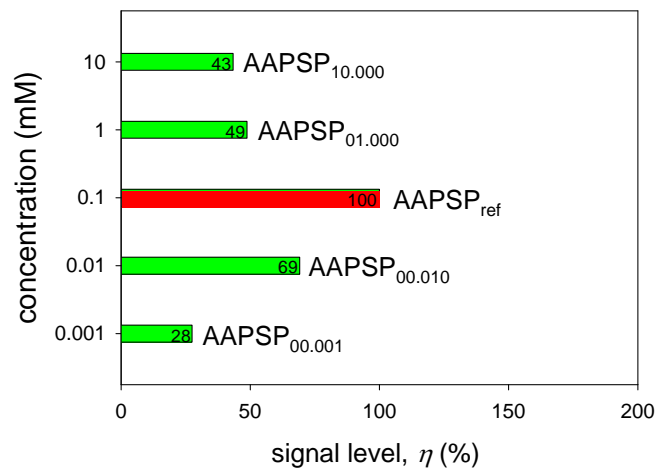
It is assumed that RuDPP remains as solution if it is dissolved well in a solvent. This assumption can be supported that *N, N*-dimethyl amide and dimethyl sulfoxide did not apply RuDPP well onto anodized aluminum. On the other hand, RuDPP applies onto anodized aluminum if it is partially dissolved in a solvent. This can be supported that toluene and water applied RuDPP onto anodized aluminum, even though these dissolved RuDPP partially. If a solvent did not dissolve RuDPP, it would not be applied onto anodized aluminum. This can be seen from the result of hexane.

As we increased the luminophore concentration from 0.001 mM to 0.1 mM,  $\eta$  increased (Figure 8 (b)). Note that the vertical axis in Figure 8 (b) was shown as log scale. The  $\eta$  was shown as a bar with the determined value. Even though we increased the concentration more than 0.1 mM,  $\eta$  decreased roughly by a half. This may be due to the concentration quenching [29]. There was an optimum concentration to maximize  $\eta$ . The maximum  $\eta$  was obtained from AAPSP<sub>00.100v</sub> whose luminophore concentration was 0.1 mM.

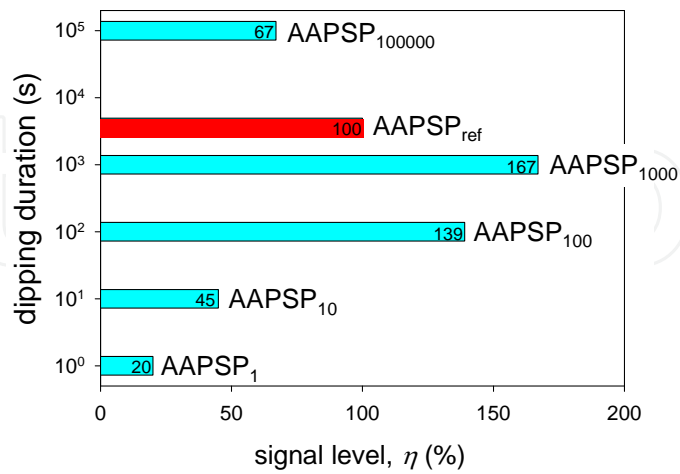
There was a peak dipping duration to maximize  $\eta$  (Figure 8 (c)). Note that the vertical axis in Figure 8 (c) was shown as log scale. The  $\eta$  was shown as a bar with the determined value. The maximum  $\eta$  was obtained from AAPSP<sub>1000v</sub> whose dipping duration was 1,000 s. For a short dipping duration, the luminophore would remain in the luminophore solution instead of applying onto the anodized surface. Roughly, the difference of  $\eta$  was a factor of 8.5 by varying the dipping duration. Even though we increased the dipping duration over 1,000 s,  $\eta$  decreased. This may be due to the concentration quenching, influencing to the luminophore application [29].



(a)



(b)



(c)

**Figure 8.** (a). Signal level,  $\eta$ , related to the polarity index. (b). Signal level,  $\eta$ , related to the luminophore concentration. (c). Signal level,  $\eta$ , related to the dipping duration

### 5.2. Pressure calibration

Figure 9 shows pressure calibrations related to the polarity index, fitted with the adsorption controlled model in Equation (4). The reference was set at atmospheric conditions. The relationship between the luminescent ratio,  $I_{ref}/I$ , and the pressure ratio,  $p/p_{ref}$  was non-linear at low pressure region. We can see that the calibration was influenced by the solvent polarity.

The pressure sensitivity,  $\sigma$ , was shown as a bar with the determined value from Equation (5) (Figure 9). The solvent polarity greatly influenced  $\sigma$ , even though the same luminophore was applied onto the same anodized aluminum. The highest  $\sigma$  of 0.62 was obtained from AAPSP<sub>ref</sub>. This showed the peak sensitivity as varying the solvent polarity. Another peak was seen at the polarity index of 10.2 (water).

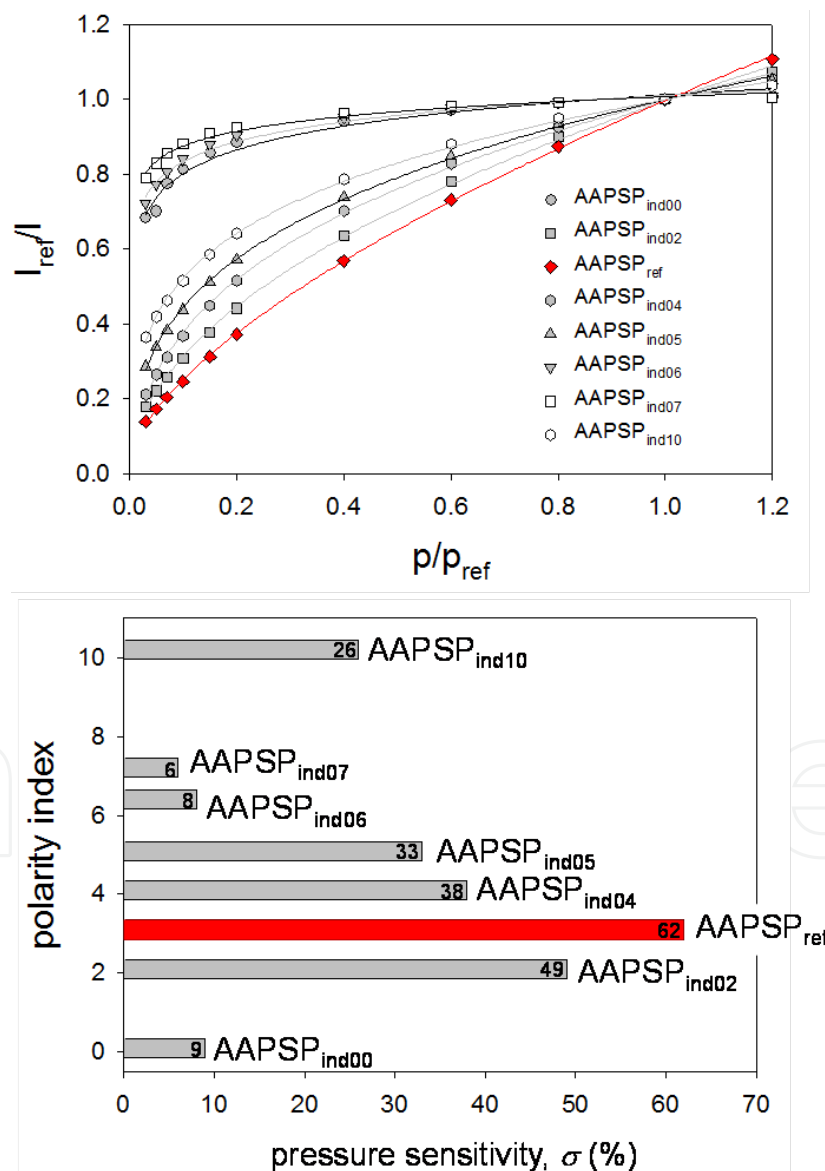


**Figure 9.** Pressure calibration and pressure sensitivity,  $\sigma$ , related to the polarity of solvent.

Figure 10 shows pressure calibrations related to the luminophore concentration, fitted with the adsorption controlled model in Equation (4). We can see two groups in calibrations: the luminophore concentration up to 0.1 mM and the concentration higher than 0.1 mM. The former showed steeper calibrations than the latter. This tells us that the former group was more pressure sensitive than the latter.

The pressure sensitivity,  $\sigma$ , was determined by using Equation (5). This value was listed in the bar scale (Figure 10). AA-PSP with the luminophore concentration up to 0.1 mM showed  $\sigma$  around 60%, while AA-PSP with higher concentration than 0.1 mM showed  $\sigma$  around 30%. This tells us that even though the amount of luminophore over 0.1 mM was dissolved in the dipping solution,  $\sigma$  did not increase. The decrease in  $\sigma$  may be due to the concentration quenching [29].

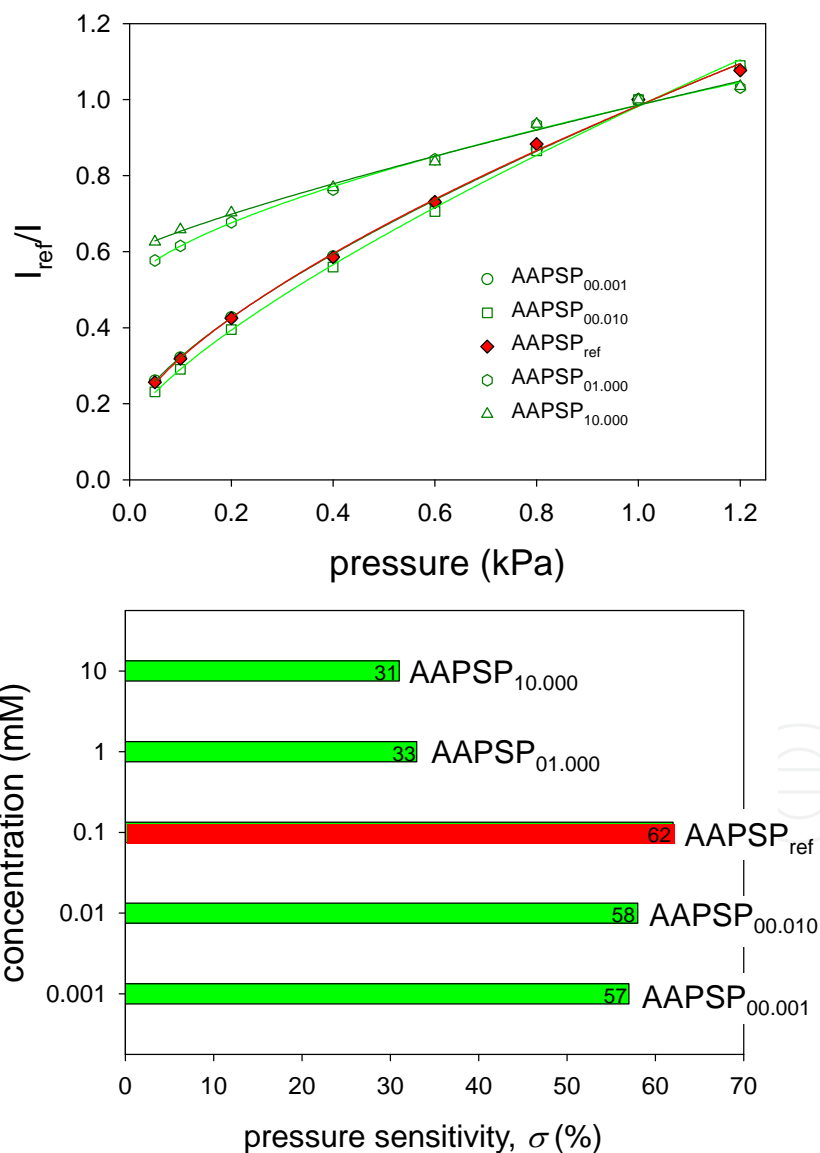


**Figure 10.** Pressure calibration and pressure sensitivity,  $\sigma$ , related to the luminophore concentration.

Figure 11 shows the pressure calibrations related to the dipping duration. The value of  $\sigma$  was determined from Equation (5). This value was shown as a bar scale in Figure 11. The maximum  $\sigma$  of 65% and the minimum  $\sigma$  of 52% were obtained from AAPSP<sub>100</sub> and AAPSP<sub>1</sub>, respectively. Even though the fifth order difference in the dipping duration was provided, a minimal effect was seen on the pressure sensitivity.

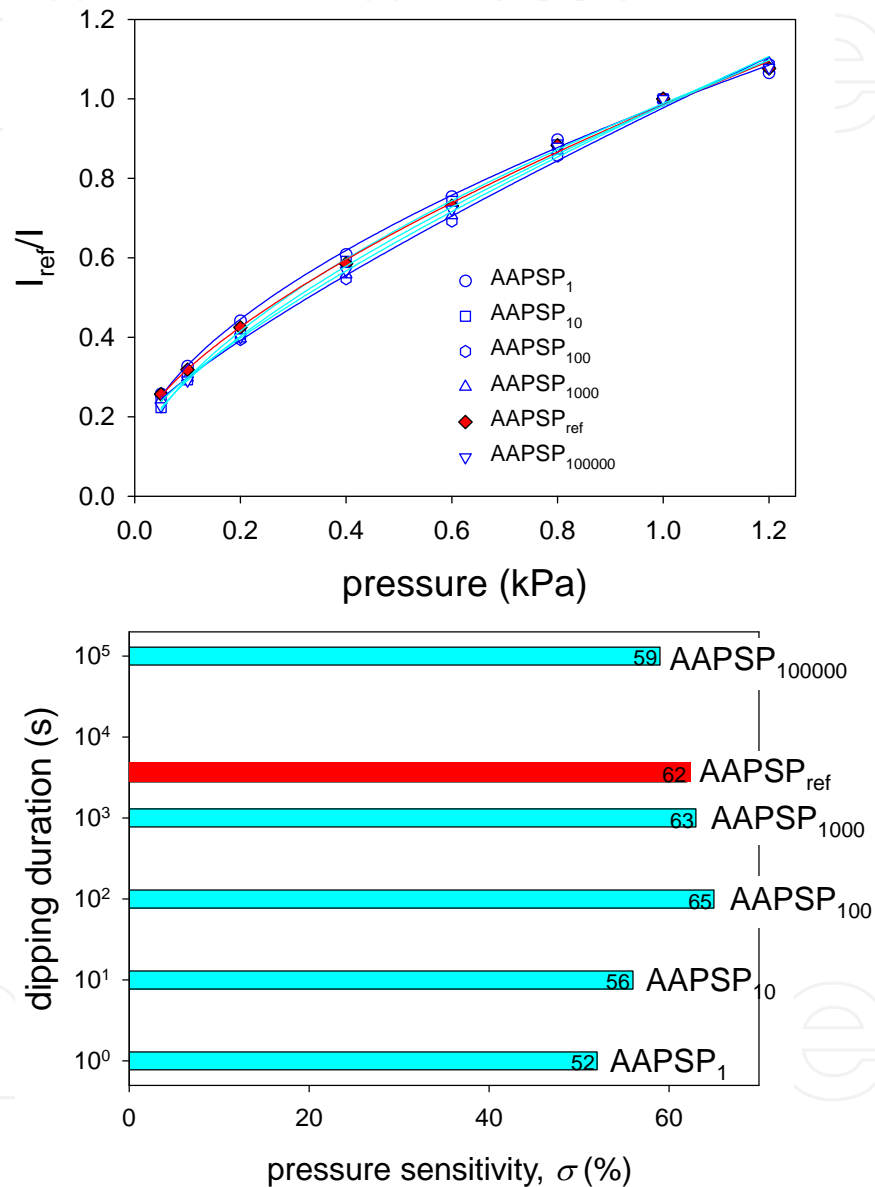


**Figure 11.** Pressure calibration and pressure sensitivity,  $\sigma$ , related to the dipping duration.

### 5.3. Temperature calibration

Figure 12 shows temperature calibrations related to the polarity index. Calibration plots were fitted with the third order polynomial described in Equation (6). We can see a monotonic decrease of the luminescent signal with increase of the temperature. The temperature depend-

ency,  $\delta$ , was determined from Equation (7), which was listed as a bar scale in Figure 12. The  $\delta$  showed a similar tendency to  $\sigma$  by varying the solvent polarity. This tells us that AA-PSP is more temperature dependent if it is more pressure sensitive.

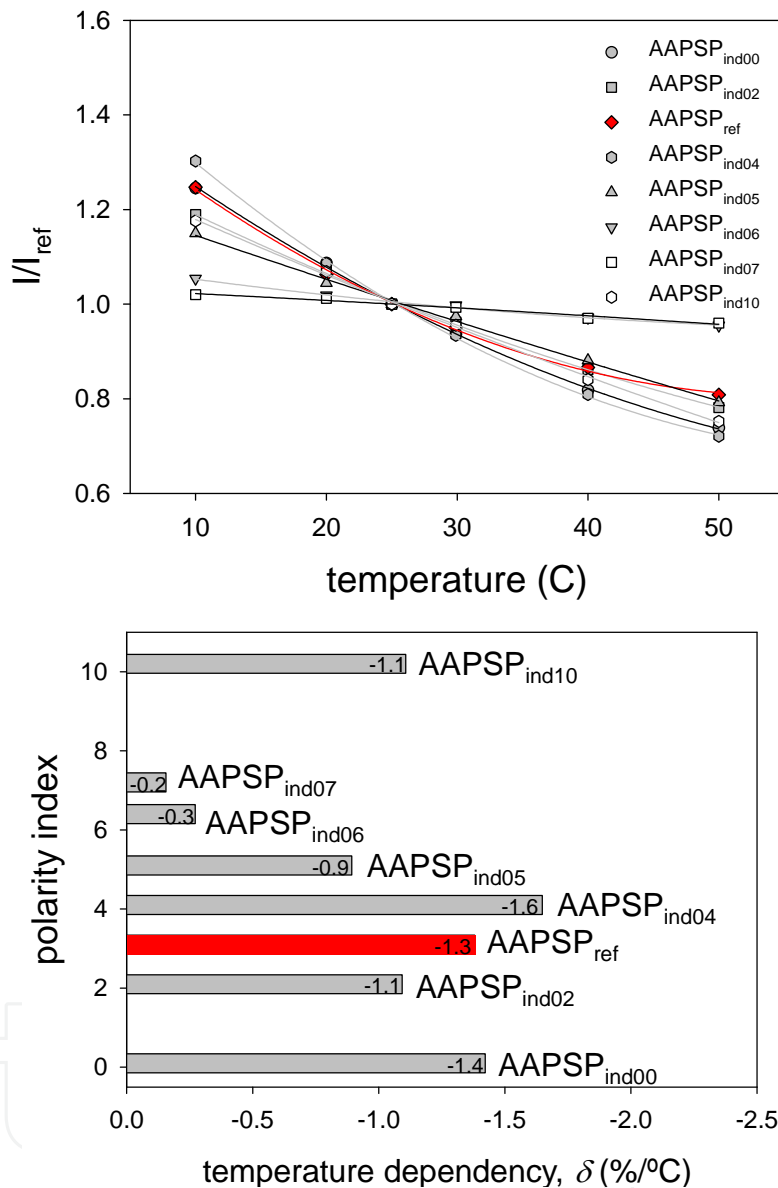


**Figure 12.** Temperature calibration and temperature dependency related to the polarity index.

Figure 13 shows temperature calibrations related to the luminophore concentration. Calibration plots were fitted with Equation (6). The calibrations show a monotonic decrease in luminescent signal as the temperature increased. As the concentration decreases, the calibrations became steep. This tells us that the temperature dependency tends to increase as the luminophore concentration decreases.

The temperature dependency,  $\delta$ , was determined from Equation (7), which was listed as a bar scale in Figure 13. As we increased the luminophore concentration,  $\delta$  decreased. Roughly,  $\delta$  became more than a half by setting the luminophore concentration from 0.001 to 10 mM.

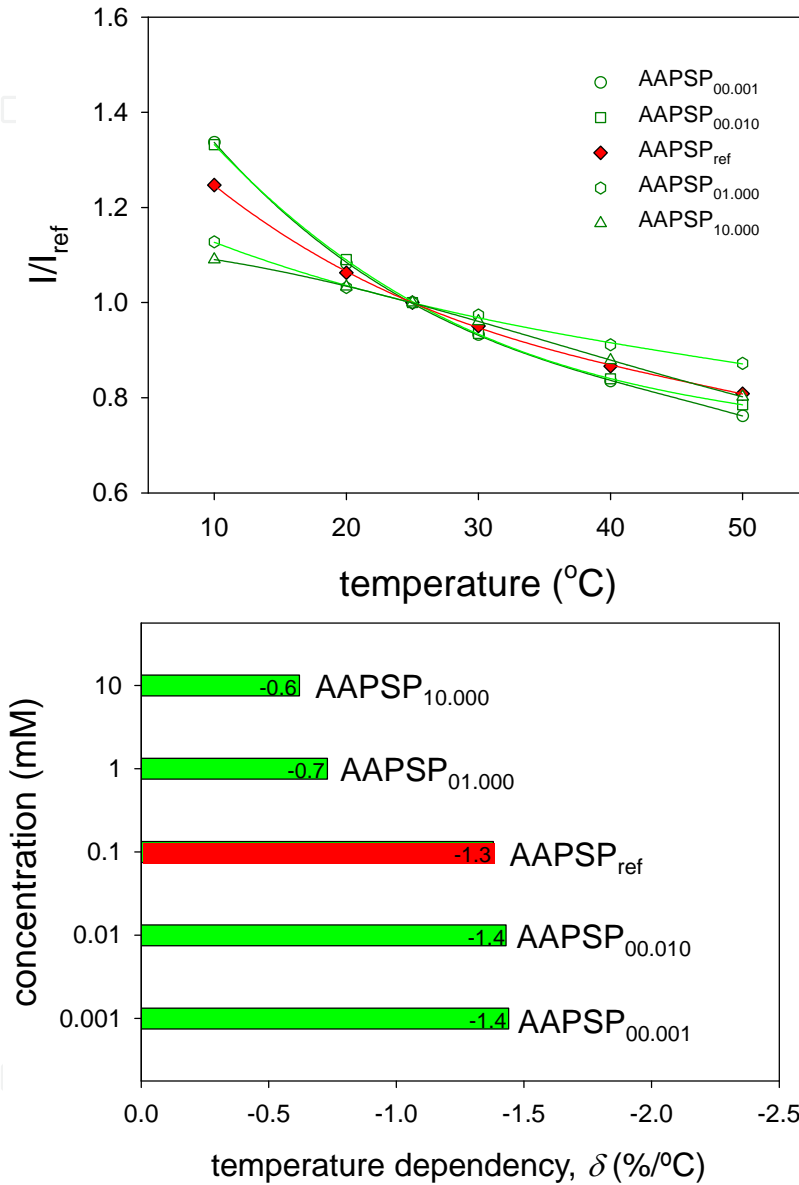


**Figure 13.** Temperature calibration and temperature dependency related to the luminophore concentration.

Figure 14 shows the temperature calibrations related to the dipping duration. The calibrations were fitted with Equation (6). The temperature calibrations showed the decrease in  $I$  with increase of the temperature.

The value of  $\delta$  was determined from Equation (7), which was listed as a bar scale in Figure 14. With increase the dipping duration, we can see that  $\delta$  decreased until 100 s and increased over this dipping duration. The difference of  $\delta$  was roughly a factor of 2. Compared to the

effect on the pressure sensitivity, the dipping duration showed a greater effect on the temperature dependency.

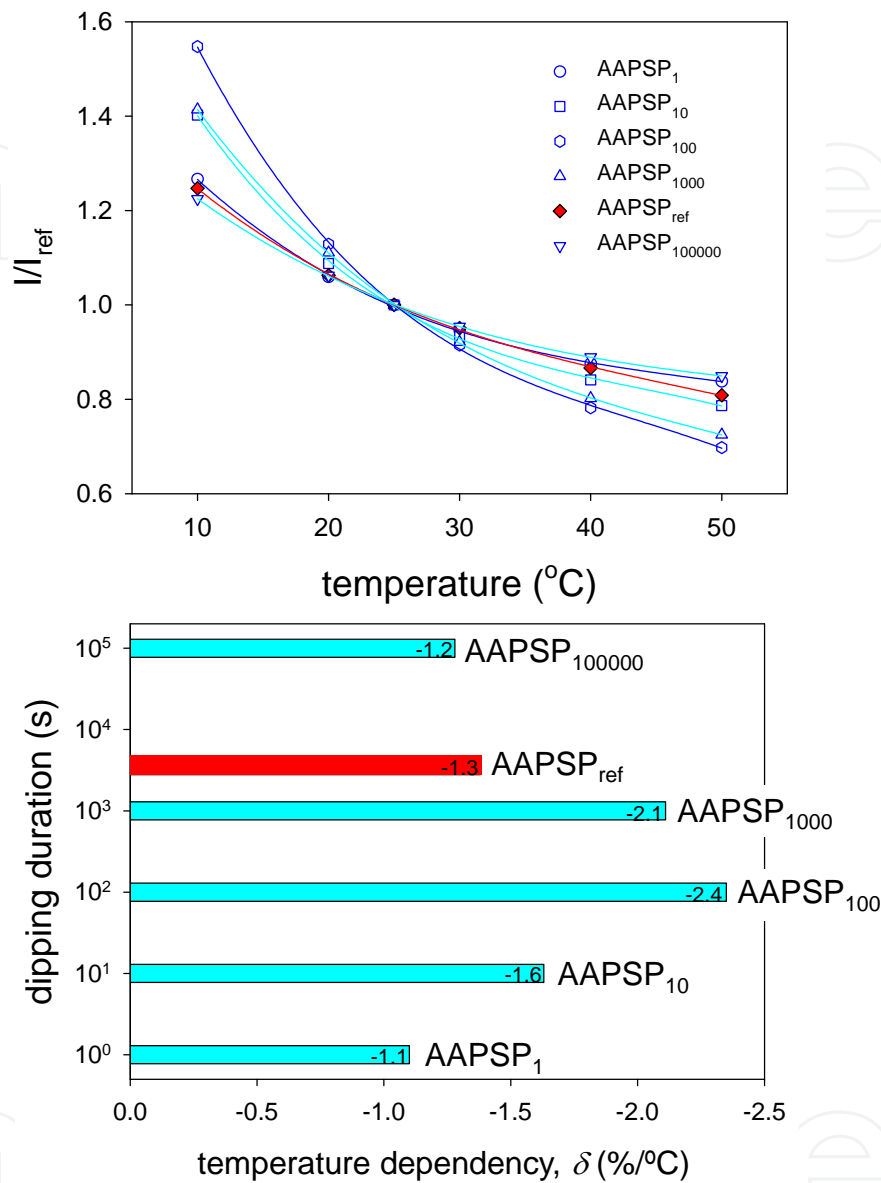


**Figure 14.** Temperature calibration and temperature dependency related to the dipping duration.

#### 5.4. Response time

A normalized step change of pressure,  $p_{norm}$ , was converted from luminescent signals through the Equation (8). Figure 15 shows response time results of AA-PSPs. Because each shock tube measurement was done by a single measurement, electrical noise with high frequency content still existed. This limited the response time characterization. The limited results were shown from the solvent polarity: AAPSP<sub>ind02</sub>, AAPSP<sub>ind03</sub>, AAPSP<sub>ind04</sub> and AAPSP<sub>ind05</sub>. These had relatively high signal levels and pressure sensitivities to separate their luminescent signal

changes from the electrical noise. Response times of AA-PSP were determined at the 90 % rise of  $p_{norm}$  (Section 4.1). The results ranged from 30 to 40  $\mu s$ . In our setup, the thickness of anodized aluminum was 10  $\mu m$ . This had  $\pm 10\%$  uncertainty from our instrument (Kett LZ-330). Kameda *et al.* reported that response time of AA-PSP is proportional to the squared value of its thickness, which corresponds to about  $\pm 20\%$  uncertainty in our measurement results [26]. Response time results were within this uncertainty, even though there were variations in step response of AA-PSPs. Considering the thickness uncertainty, response times of AA-PSPs can be said on the order of ten microseconds with the anodized-aluminum thickness of 10  $\mu m$ . Sakaue *et al.* reported that the response time of AA-PSP showed a minimal effect by the luminophore selected [31]. This indicates that the response time of AA-PSP has smaller effect on the luminophore application parameters than the effect on AA-PSP thickness.

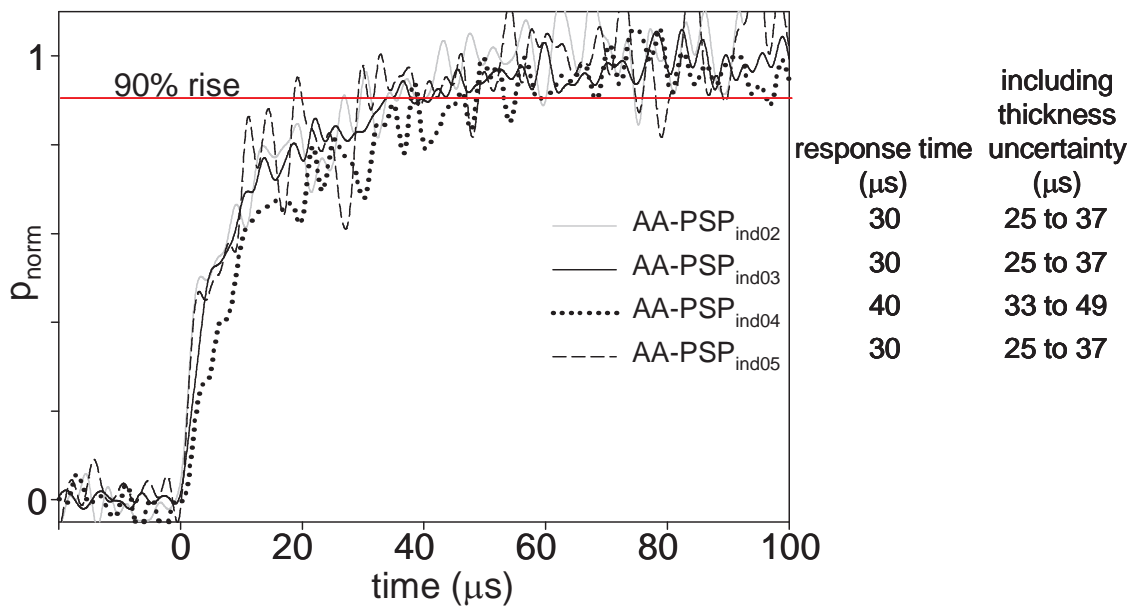


Figure 15. Response time results related to the solvent polarity.

## 6. Discussion: AA-PSP characterizations related to Luminophore Application Parameters

Table 2 lists the maximum and minimum values of AA-PSP characterizations: signal level, pressure sensitivity, and temperature dependency. The signal level was greatly influenced by varying the solvent polarity. The difference was a factor of 14.5. The second largest effect was the dipping duration. The difference in the signal level was a factor of 8.4. The luminophore concentration influenced the signal level for a factor of 3.6. Overall, the signal level was most influenced by the luminophore-application parameters.

The pressure sensitivity was greatly influenced by the solvent polarity. The difference in the sensitivity was a factor of 10.3. By varying the luminophore concentration, the difference was

a factor of 2. The difference was a factor of 1.2 by varying the dipping duration. Among the dipping parameters, the pressure sensitivity was most influenced by the solvent polarity.

The temperature dependency was greatly influenced by the solvent polarity. The difference was a factor of 8. The differences by the luminophore concentration and the dipping duration were on the same order, which was a factor of 2. The temperature dependency was influenced by the dipping parameters, but the change was not as large as that of the pressure sensitivity. Overall, the solvent polarity influenced the most of the AA-PSP characterizations.

	Solvent Polarity		Luminophore Concentration		Dipping Duration	
	max.	min.	max.	min.	max.	min.
$\eta$ (%)	189	13	100	27.5	167.1	20.1
$\sigma$ (%)	62	6	62	31	65	52
$\delta$ (%/°C)	-0.2	-1.6	-0.6	-1.4	-1.1	-2.4

**Table 2.** The maximum and minimum AA-PSP characterizations.

## 7. Conclusions

The luminophore application method of dipping deposition was studied to provide the relationship between this method and AA-PSP characterizations for fabricating an optimized optical pressure sensor for unsteady aerodynamic applications. The characterizations were the signal level, pressure sensitivity, temperature dependency, and response time. Three important parameters in the luminophore application method were studied: solvent polarity, luminophore concentration, and dipping duration. It was found that the AA-PSP characterizations were related to one another. Therefore, an absolute optimization of the luminophore application method was not obtained. However, the relationship among these characterizations and the luminophore-application parameters were revealed, which were concluded as follows.

The solvent polarity was the most influencing parameter. The signal level showed the widest range from 13% to 189% compared to the signal level of the reference AA-PSP (100%). The pressure sensitivity ranged from 6 to 62 %, and the temperature dependency from -0.2 to -1.6 %/°C. It was seen that the pressure-sensitive AA-PSP was also temperature sensitive. It was shown qualitatively by photograph that the solubility was related to the solvent polarity. Well luminophore-dissolved solvents did not show higher AA-PSP outputs. This may be that the luminophore remained in the solvent and was not applied onto the anodized-aluminum surface well.

The luminophore concentration and dipping duration greatly influenced to the signal level. However, the influence to the pressure sensitivity and the temperature dependency was relatively small. The difference was less than or equal to a factor of 2.

The effect of AA-PSP response time due to the dipping deposition method was smaller than the effect by the thickness uncertainty of AA-PSP. With the anodized-aluminum thickness of 10  $\mu\text{m}$ , the response time characterization was within the thickness uncertainty. The response time was on the order of ten microseconds.

## Acknowledgements

The author would like to thank his colleagues for technical supports: Dr. K. Morita (JAXA), Mr. Y. Iijima (JAXA), Ms. K. Ishii (The University of Tokyo), Mr. Y. Yamada (The University of Electro-Communications), and Prof. Y. Sakamura (Toyama Prefectural University).

## Author details

Hiroataka Sakaue\*

Address all correspondence to: [sakaue@chofu.jaxa.jp](mailto:sakaue@chofu.jaxa.jp)

Institute of Aeronautical Technology, Japan Aerospace Exploration Agency / Chofu, Tokyo, Japan

## References

- [1] Nakakita K, *et al.* 2000. AIAA2000-2523.
- [2] Nakakita K, Asai K. 2002. AIAA2002-2911.
- [3] Ishiguro Y, *et al.* 2007. AIAA2007-01187.
- [4] Miyamoto K, *et al.* 2010. AIAA2010-4798.
- [5] Morita K, *et al.* 2011. AIAA2011-3724.
- [6] Disotell KJ, Gregory JW. 2011. Rev. Sci. Instrum. 82:075112.
- [7] Disotell KJ, *et al.* 2012. AIAA2012-2757.
- [8] Yang L, *et al.* 2012. Int. J. Heat Fluid Flow 37: 9 – 21.
- [9] Yang L, *et al.* 2012. Sens. Actuators B 161:100 – 7.
- [10] Yang L, *et al.* 2012. Exp. Therm. Fluid Sci. 40:50 –56.
- [11] Hayashi T, *et al.* 2012. 28th International Symposium on Shock Waves, Vol. 1, ISBN 978-3-642-25687-5, pp. 607 – 613.

- [12] Fujii S, *et al.* 2013. AIAA2013-0485.
- [13] McGraw CM, *et al.* 2003. *Rev. Sci. Instrum.* 74:5260-66.
- [14] Virgin CA, *et al.* 2005. *Proc. 2005 ASME Int. Mech. Eng. Congr. Expo.*, pp. 297-307.
- [15] McGraw CM, *et al.* 2006. *Exp. Fluids* 40:203-11.
- [16] Nakakita K. 2007. AIAA2007-3819.
- [17] Nakakita K, Arizono H. 2009. AIAA2009-3847.
- [18] Klein C, *et al.* 2010. *Numerical and Experimental Fluid Mechanics VII*, pp. 323-30.
- [19] Yorita D, *et al.* 2010. AIAA2010-0307.
- [20] Asai K, Yorita D. 2011. AIAA2011-0847.
- [21] Nakakita K, *et al.* 2012. AIAA2012-2758.
- [22] Steimle PC, *et al.* 2012. *AIAA J.* 50:399-415.
- [23] Watkins AN, *et al.* 2012. AIAA2012-2756.
- [24] Wong OD, *et al.* 2012. *Proc. 68th Am. Helicopter Soc. Annu. Forum Technol. Disp., Pap.* AHS2012-000233.
- [25] Mérienne MC, *et al.* 2013. AIAA2013-1136.
- [26] Kameda, M.; Tezuka, N.; Hangai, T.; Asai, K.; Nakakita, K.; Amao, M. *Meas. Sci. Technol.* 2004, 15, 489–500.
- [27] Sakaue, H. *Rev. Sci. Instrum.* 2005, 76, 084101.
- [28] Liu, T.; Guille, M.; Sullivan, J.P. Accuracy of Pressure Sensitive Paint. *AIAA J.* 2001 40, 103–112.
- [29] Lakowicz, J.R. *Principles of Fluorescence Spectroscopy*. Kluwer Academic/Plenum Publishers: New York, NY, USA, 1999; Chapter 1.4.A.
- [30] Liu, T.; Sullivan, J.P. *Pressure and Temperature Sensitive Paints*; Springer Verlag: Heidelberg, Germany, 2004; pp. 27–31 and Chapter 7.
- [31] Sakaue, H., Morita, K., Iijima, Y., Sakamura, Y., *Sensors and Actuators A: Physical*, Elsevier, Vol. 199, No. 1, pp. 74 – 79, 2013.